A Diverse Range of Hemozoin Inhibiting Scaffolds Act on *Plasmodium falciparum* as Heme Complexes

Roxanne Openshaw,[†] Keletso Maepa,[‡] Stefan J. Benjamin,[†] Lauren Wainwright,[†] Jill M. Combrinck,[‡] Roger Hunter[†] and Timothy J. Egan*[†,ǁ]

[†]Department of Chemistry, University of Cape Town, Private Bag Rondebosch, Cape Town 7701, South Africa [‡]Division of Clinical Pharmacology, Department of Medicine and [ǁ]Institute of Infectious Disease and Molecular Medicine, University of Cape Town, Observatory, Cape Town 7925, South Africa

Corresponding Author

*E-mail: timothy.egan@uct.ac.za

Supporting Information

Table S1: β-hematin inhibition and parasite growth inhibition IC_{50} values in the NF54 strain for the compounds investigated in this study.

Scaffold	Compound	β-hematin inhibition IC_{50} (μM)	NF54 parasite IC_{50} (μM)
Quinolines	**1**	31.5 ± 0.5[1]	0.0190 ± 0.0004
	2	17 ± 2	0.0204 ± 0.0007
Benzamides	**3**	13 ± 1[1]	5.0 ± 1.0[1]
	4	6.8 ± 0.1[1]	0.6 ± 0.1
	5	> 1000[1]	8.1 ± 0.5
Triarylimidazoles	**6**	13.8 ± 0.4[2]	1.8 ± 0.1
	7	14.6 ± 0.2[2]	7.0 ± 0.1
	8	19 ± 1[2]	15 ± 4
	9	> 1000[2]	4.2 ± 0.1
Quinazolines	**10**	20 ± 2	0.189 ± 0.006
	11	23 ± 2	0.29 ± 0.02
	12	26 ± 3	0.240 ± 0.008
Benzimidazoles	**13**	32 ± 1[3]	0.62 ± 0.05
	14	24 ± 4[3]	1.3 ± 0.2
	15	38 ± 1[3]	15.0 ± 0.3
	16	15.6 ± 0.5[3]	2.3 ± 0.6
Benzothiazole	**17**	30 ± 2	1.50 ± 0.02
Benzoxazole	**18**	22 ± 1	7.49 ± 0.06

Table S2: Exchangeable heme (fmols heme per cell) at the IC_{50} and cellular accumulation ratios (CAR ± SD) for compounds investigated in this study. Amounts of accumulated active compounds are given by IC_{50} × CAR × mean volume of the infected RBC (V_{cell}).

Scaffold	Compound	Heme (fmol/cell)	CAR	IC_{50} × CAR × V_{cell} (fmol/cell)[a]
quinoline	**1**	0.15 ± 0.02	105 342 ± 3 365[4]	0.17 ± 0.01
	2	0.14 ± 0.02	98 024 ± 15 296[4]	0.18 ± 0.03
benzamide	**4**	0.29 ± 0.05	5 934 ± 945	0.30 ± 0.07
triarylimidazole	**6**	0.26 ± 0.09	479 ± 223	0.07 ± 0.03
quinazoline	**10**	0.050 ± 0.007	1 757 ± 242	0.028 ± 0.004
	11	0.062 ± 0.007	1 746 ± 206	0.042 ± 0.006
	12	0.08 ± 0.02	1 823 ± 381	0.037 ± 0.008
benzimidazole	**13**	0.23 ± 0.03	5 305 ± 1 079	0.27 ± 0.06
	14	0.33 ± 0.01	1 912 ± 276	0.20 ± 0.04
	16	0.52 ± 0.02	2 039 ± 757	0.4 ± 0.2
benzothiazole	**17**	0.25 ± 0.03	1 599 ± 552	0.20 ± 0.07

[a]V_{cell} for a parasitized RBC = 84 ± 6 fL;[5]

Table S3. Statistical measures of difference between Raman spectra based on separation of centroids between clusters in PCA using Welch's t-test.

Spectrum of component 1	Spectrum of component 2	P	R^2
Putative heme-**13** complex in parasite	oxyhemoglobin	< 0.0001	0.6082
	deoxyhemoglobin	< 0.0001	0.7523
	hemozoin	< 0.0001	0.7729
	hemin	< 0.0001	0.6017
	hematin	< 0.0001	0.8267
	13	< 0.0001	0.8889
	synthetic hemin-**13** complex	0.8043	0.0005
Hemozoin	oxyhemoglobin	< 0.0001	0.8364
	deoxyhemoglobin	< 0.0001	0.8887
	hemin	< 0.0001	0.8349
	hematin	< 0.0001	0.8104
	13	< 0.0001	0.8551
	β-hematin	0.8528	0.0001
Oxyhemoglobin	deoxyhemoglobin	< 0.0001	0.8941
	hemin	< 0.0001	0.3933
	hematin	< 0.0001	0.3467
	13	< 0.0001	0.6501

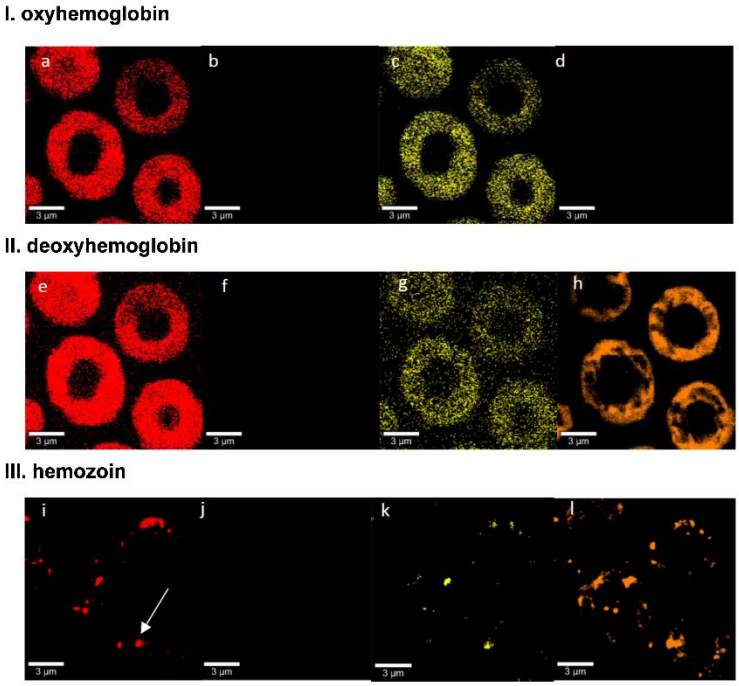

Figure S1. Confocal Raman true mapping images, obtained using true component analysis and filter viewer tools, for untreated infected RBCs. Cells contain three distinct Fe(III)PPIX complexes: (I) oxyhemoglobin, (II) deoxyhemoglobin and (III) hemozoin which were imaged at specific Raman peaks using the filter viewer tool: a, e and i) 754 cm^{-1} (red); b, f and j) 1080 cm^{-1} (green); c, g and k) 1090 cm^{-1} (yellow) and; d, h and l) 1642 cm^{-1} (orange). These peaks have previously been assigned respectively to ν_{15} (ν(pyrrole breathing)$_{asym}$), ν_{23} ($\nu(C_\beta C_1)_{asym}$), ν_{23} ($\nu(C_\beta C_1)_{asym}$ and/or $\gamma(=C_\beta H_2)_{sym}$) and ν_{10} ($\nu(C_\alpha C_m)_{asym}$).[6-9] 15 × 15 points per image and points per line and 0.05 s integration time with a run time = 35 min. Note the absence of a signal at 1080 cm^{-1} for any of these Fe(III)PPIX species. White arrows indicate probable extracellular hemozoin crystals probably arising from limited cell lysis during sample preparation.

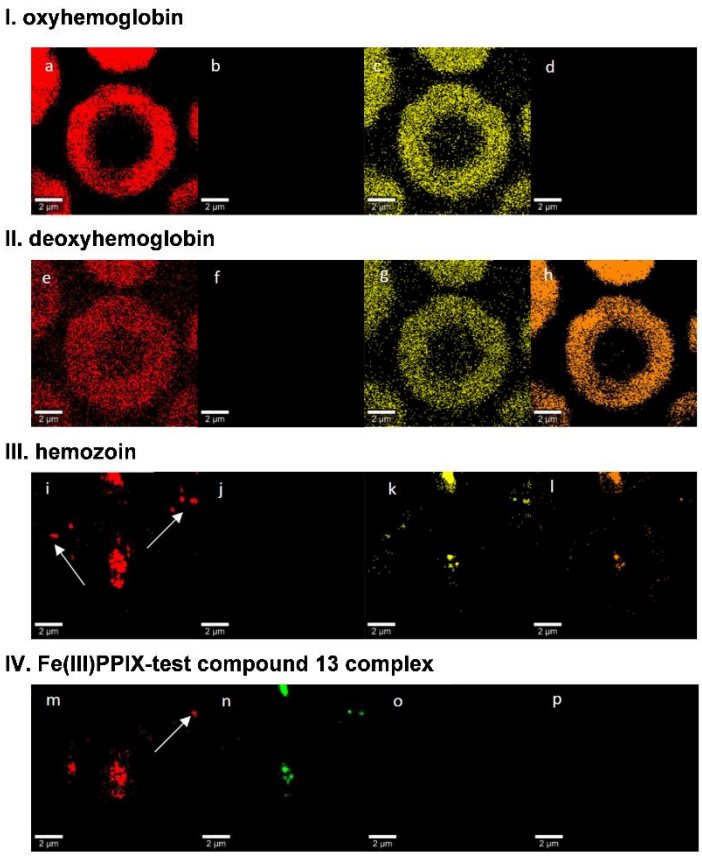

Figure S2. Confocal Raman true mapping images obtained, using true component analysis and filter viewer tools, for test compound **13**-treated infected RBCs. The cells contained four distinct Fe(III)PPIX complexes: (I) oxyhemoglobin, (II) deoxyhemoglobin, (III) hemozoin and (IV) Fe(III)PPIX-test compound **13** complex which were imaged at specific Raman peaks using the filter viewer tool: a, e, i and m) 754 cm^{-1} (red); b, f, j and h)1080 cm^{-1} (green); c, g, k and o) 1090 cm^{-1} (yellow) and; d, h, l and p) 1642 cm^{-1} (orange). 15 × 15 points per image and points per line and 0.05 s integration time with a run time = 35 min. White arrows indicate probable extracellular hemozoin crystals.

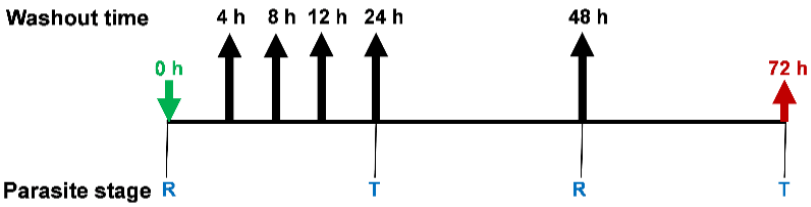

Figure S3. Strategy of the speed of killing experiment: 0 h = time of inoculation, 72 h = time of assay, R = ring stage, T = trophozoite, washout times indicated by black arrows.

1. Wicht, K. J.; Combrinck, J. M.; Smith, P. J.; Hunter, R.; Egan, T. J., Identification and SAR evaluation of hemozoin-inhibiting benzamides active against *Plasmodium falciparum*. *J. Med. Chem.* **2016,** *59*, 6512-6530.

2. Wicht, K. J.; Combrinck, J. M.; Smith, P. J.; Hunter, R.; Egan, T. J., Identification and mechanistic evaluation of hemozoin-inhibiting triarylimidazoles active against *Plasmodium falciparum*. *ACS Med. Chem. Lett.* **2017,** *8*, 201-205.

3. L'abbate, F. P.; Müller, R.; Openshaw, R.; Combrinck, J. M.; de Villiers, K. A.; Hunter, R.; Egan, T. J., Hemozoin inhibiting 2-phenylbenzimidazoles active against malaria parasites. *Eur. J. Med. Chem.* **2018,** *159*, 243-254.

4. Wicht, K. J. Discovery of benzamides and triarylimidazoles active against *Plasmodium falciparum* via haemozoin inhibition: high throughput screening, synthesis and structure-activity relationships. University of Cape Town https://open.uct.ac.za/handle/11427/16939, 2015.

5. Okafur, U. E.; Tsoka-Gwegweni, J. M.; Bibirigea, A.; Irimie, A.; Tomuleasa, C., Parasitaemia and haematological changes in malaria-infected refugees in South Africa. *S. Afr. Med. J.* **2016,** *106*, 413-416.

6. Wood, B. R.; Langford, S. J.; Cooke, B. M.; Glenister, F. K.; Lim, J.; McNaughton, D., Raman imaging of hemozoin within the food vacuole of *Plasmodium falciparum* trophozoites. *FEBS Lett.* **2003,** *554*, 247-252.

7. Webster, G. T.; Tilley, L.; Deed, S.; McNaughton, D.; Wood, B. R., Resonance Raman spectroscopy can detect structural changes in haemozoin (malaria pigment) following incubation with chloroquine infected erythrocytes. *FEBS Lett.* **2008,** *582*, 1087-1092.

8. Abe, M.; Kitagawa, T.; Kyogoku, Y., Resonance Raman spectra of octaethylporphyrinatonickel(II) and meso-deuterated and nitrogen-15 substituted derivatives. II. A normal coordinate analysis *J. Chem. Phys.* **1978,** *69*, 4526-4534.

9. Hu, S.; Smith, K. M.; Spiro, T. G., Assignment of protoheme resonance Raman spectrum by heme labeling in myoglobin. *J. Am. Chem. Soc.* **1996,** *118*, 12638-12646.